Neutral Current and Charged Current Results from H1

Beate Heinemann

DESY, Hamburg

On behalf of the

H1 Collaboration

DIS 98, Brussels, April 7^{th}, 1998

Deep Inelastic Scattering

$e^+p \longrightarrow e^+X,\ \bar{\nu}X$

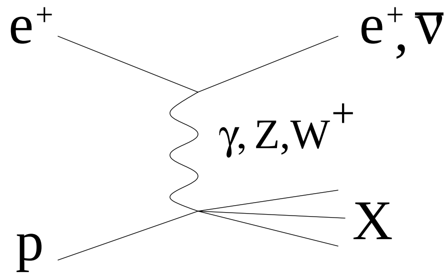

kinematic variables:

$Q^2 = -(k - k')^2 = xys$

$x_{Bj} = \frac{Q^2}{2P\cdot q}$

$y = \frac{P\cdot q}{P\cdot k}$

$M = \sqrt{xs}$

HERA: $E_e = 27.6$ GeV, $E_p = 820$ GeV $\Rightarrow \sqrt{s} \simeq 300$ GeV

probe proton at very short distances via

t-channel exchange of virtual gauge boson

- measurement of proton Structure
- Test of pQCD up to very high Q^2
- Test of EW Standard Model

total luminosity for e^+p data 37 pb^{-1}

- In situ Energy Calibration
- Update of High Q^2 Results (DESY-97-24)
- Neutral Current cross sections at High Q^2
- Charged Current cross sections at High Q^2

H1 detector

Liquid Argon Calorimeter: 45000 cells

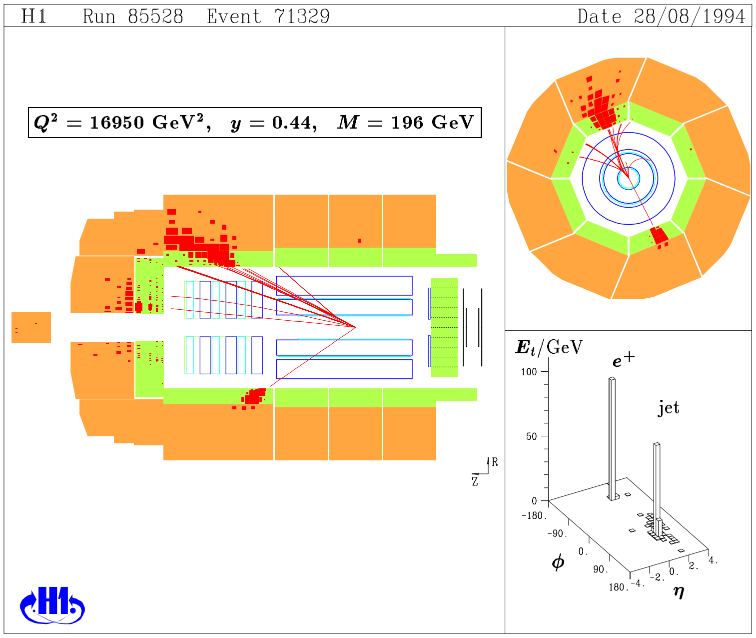

EM section

$\sigma(E)/E = 12\%/\sqrt{E} \oplus 1\%$

syst. Unc.: 1 $\Leftrightarrow$3%

HAD section

$\sigma(E)/E = 50\%/\sqrt{E} \oplus 1\%$

syst. Unc.: 3 $\Leftrightarrow$4%

Observables in NC events:

E_e and θ_e of the electron

$\Sigma = E - p_z$ and $P_{t,h}$ of the hadrons

$\Longrightarrow$ various possibilities for reconstruction of kinematics with different systematics

Kinematic Reconstruction

Methods used for Measurements:

- Electron Method: $y_e = 1 \Leftrightarrow \frac{E'_e}{E_e} \sin^2 \frac{\theta_e}{2}$ $Q^2_e = 4E'_e E_e \cos^2 \frac{\theta_e}{2}$
  - most precise at high y / low x
  - bad x resolution at low y
  - good Q^2 resolution in full range
- Hadron Method: $y_h = \frac{\Sigma}{2E_e}$ $Q^2_h = \frac{p^2_{t,h}}{1-y_h}$
  - low precision, but only method for charged current
- $e\Sigma$ Method: $x_{e\Sigma} = x_\Sigma$ and $Q^2_{e\Sigma} = Q^2_e$
  - precise over the whole kinematic range
  - good resolution even at very high x

Further Methods for Calibration and Cross Checks

- Σ Method:
  - good x resolution also at low y
  - independent of QED initial state radiation
- Double Angle Method:
  - angle of scattered electron and hadronic final state
  - high precision at high Q^2, but sensitive to QED radiation
  - independent of energy scale $\Rightarrow$ used for calibration
- ω Method:
  - identification/correction of radiative events
  - determination of kinematics/calibration on an event by event basis

Electron Energy Calibration

- Detailed calibration performed in backward part of LAr calorimeter $\theta > 80^o$:
  - at low $y < 0.3$ using the Double Angle method (independent of electron energy) as reference
  - $E_{DA} = \frac{2E_{e,beam}\sin\gamma}{\sin\gamma + \sin\theta_e - \sin(\gamma+\theta_e)}$
  - cm-wise in z and octant by octant in ϕ

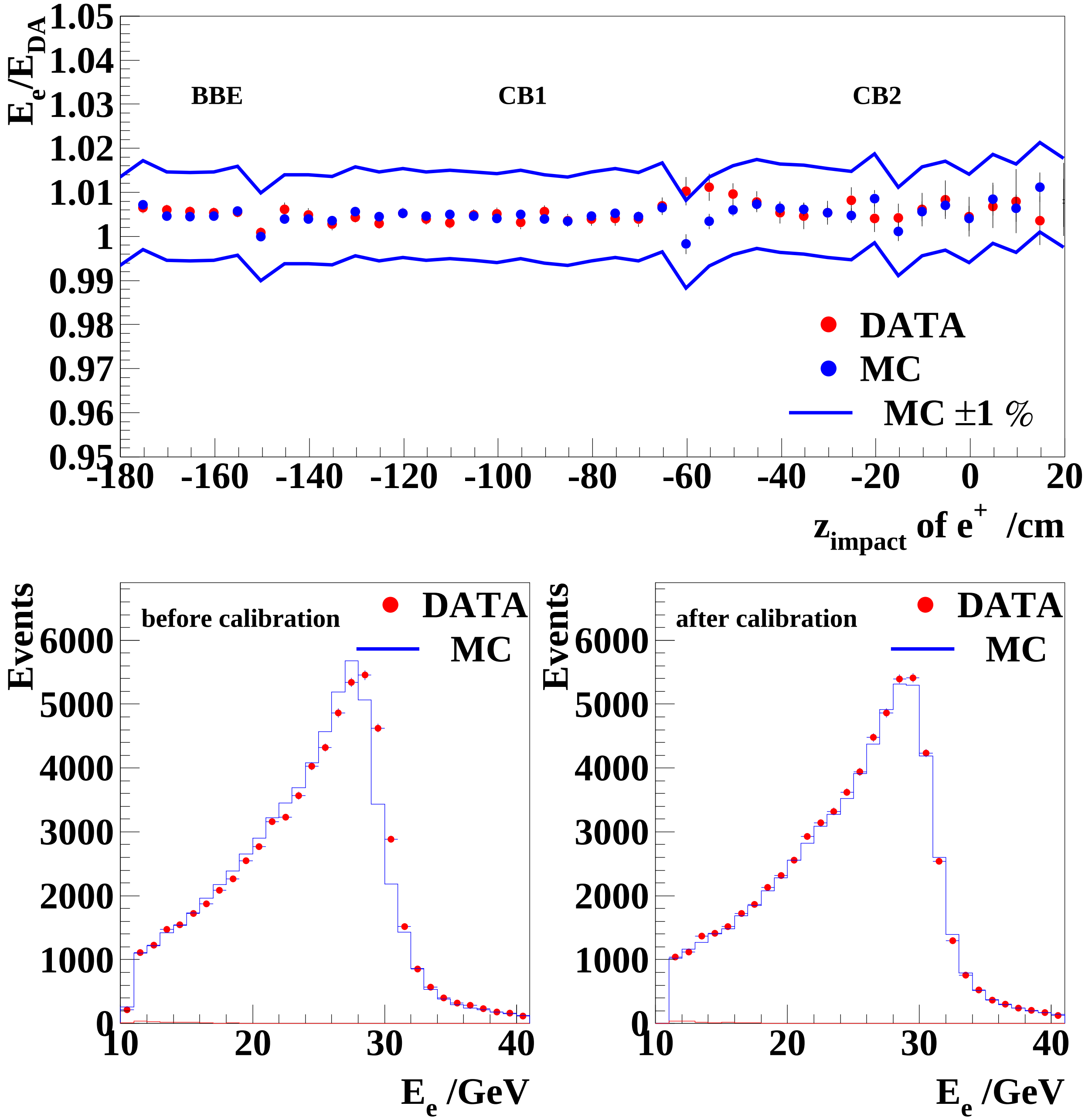

- reduction of energy scale uncertainty to $< 1\%$

Electron Energy Calibration

Improvement of the electron energy calibration using different types of events

- NC DIS events (DA-method and ω-method)
- elastic QED Compton and $e^+p \rightarrow e^+e^-e^+p$

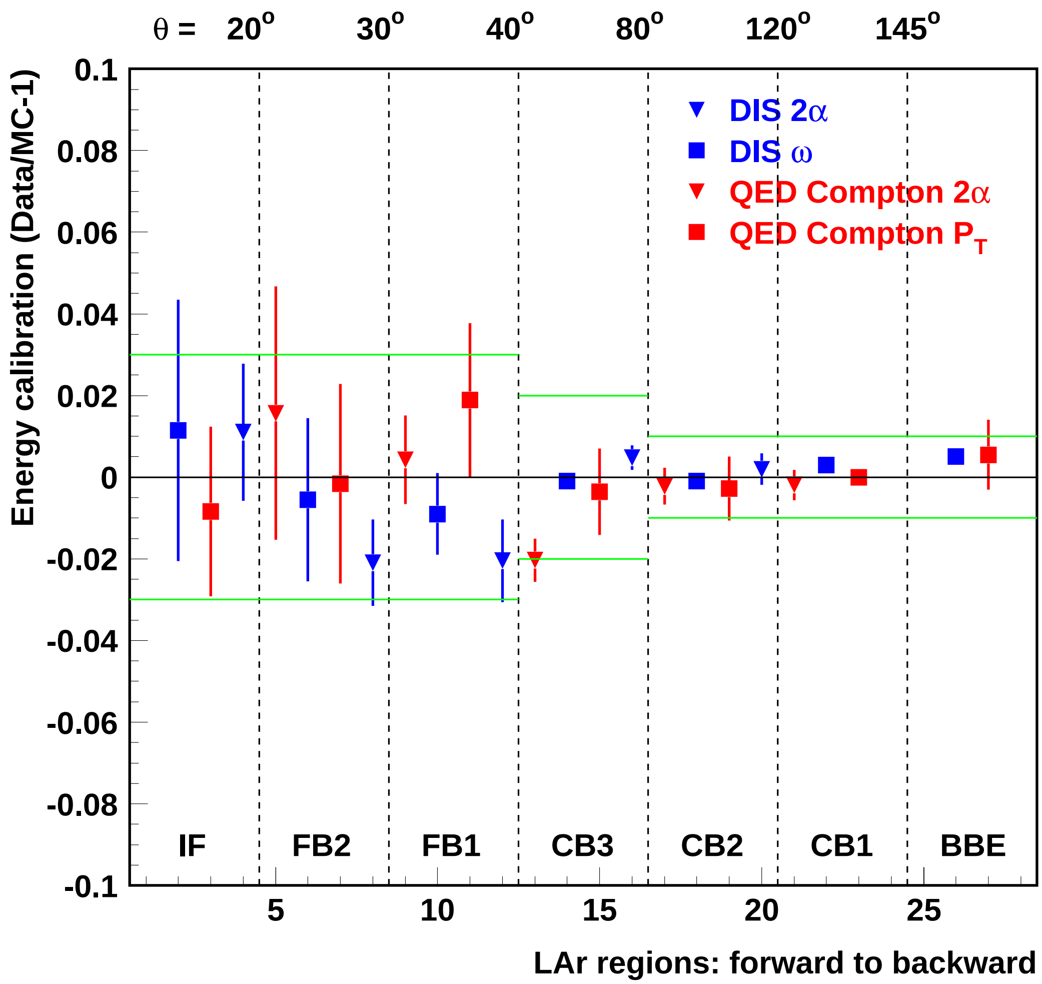

- e-calib. well within originally quoted $\pm 3\%$ syst. for central LAr wheels
  $\Rightarrow$ 1% precision for θ between 80° to 150° ($Q^2 < 1000$ GeV^2)
- In the forward LAr wheels ($Q^2 > 2500$ GeV^2):
  consistency from various methods using NC DIS and QED
  $\Rightarrow$ calibration scale improved.
  Uncertainty at the 3% precision level only limited by statistics

Hadronic Energies

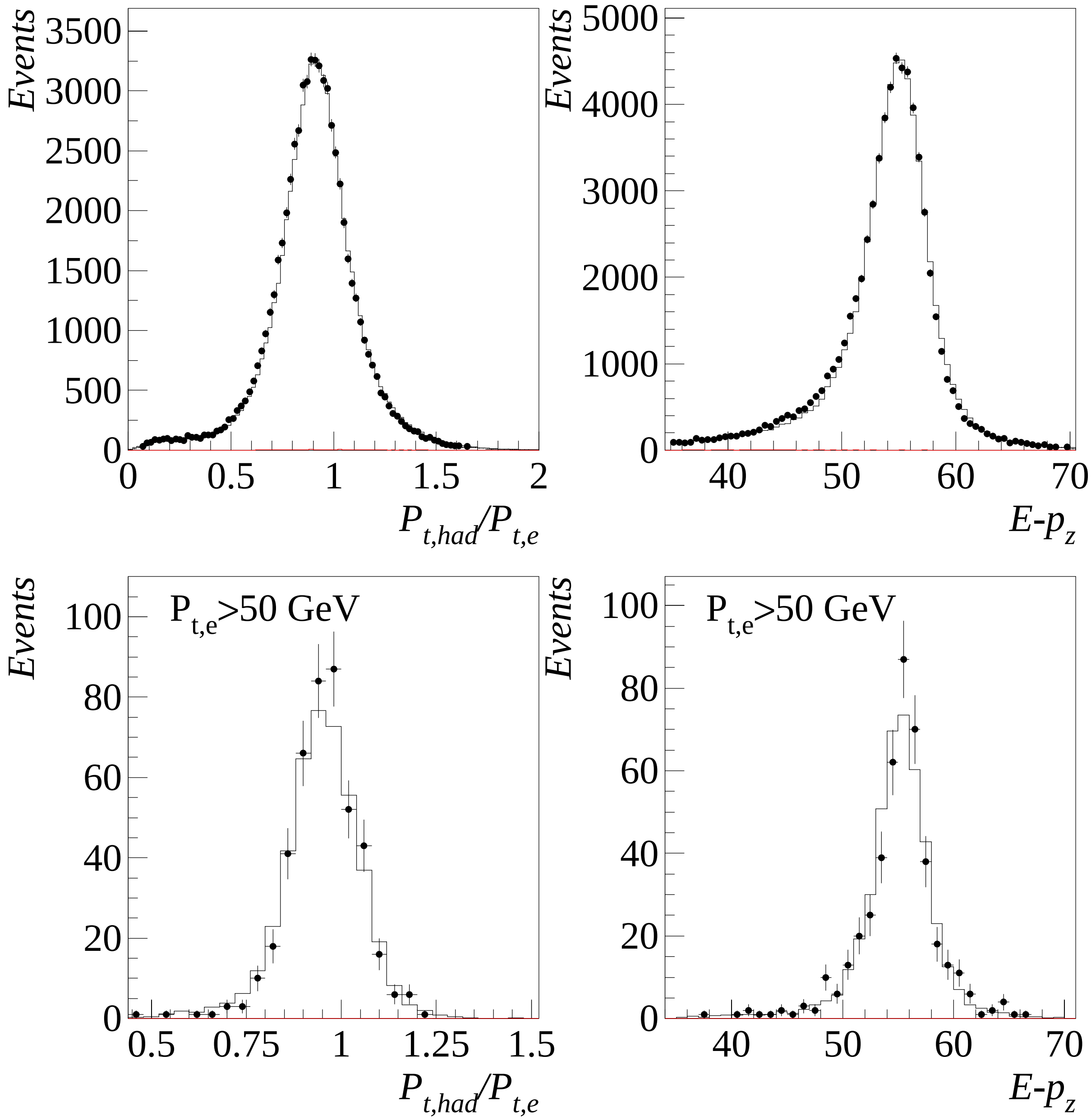

- hadronic scale is being precisely calibrated using the P_t balance of the hadrons and the electron in NC events as reference
- width and scale of the hadronic distributions well described at low and high P_t

P_t balance vs. Q^2

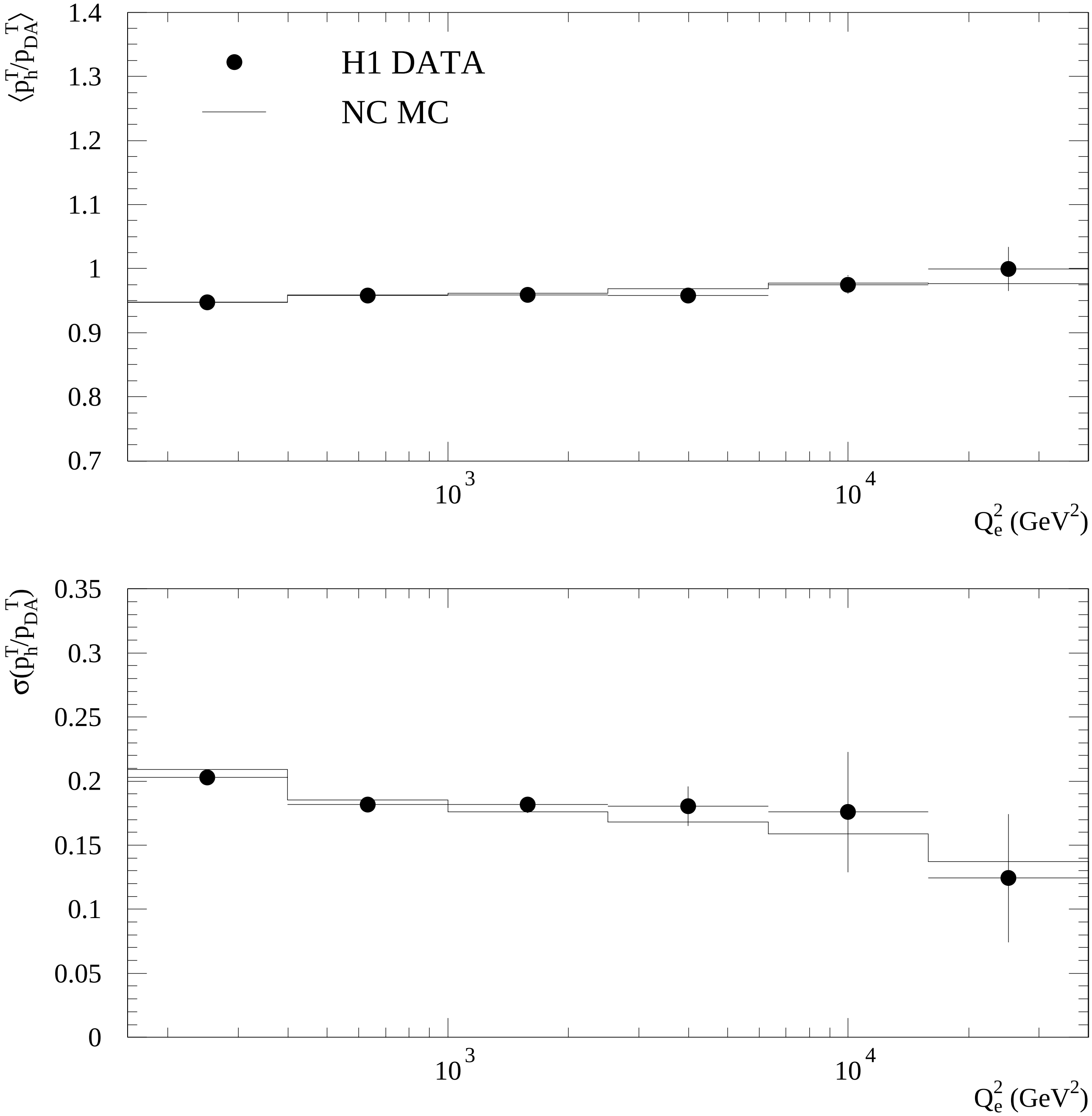

- reduction of systematic error on hadronic energy scale $4 \rightarrow 3\%$ in forward region ($\gamma < 60^o$)
- mean of P_t balance well described
- resolution $\simeq 20\%$ in $P_t \Longrightarrow Q^2$ resolution $\simeq 30\%$

Update on Very High Q^2 results with 97 data

- New E_e calibration
- Slightly modified selection cuts

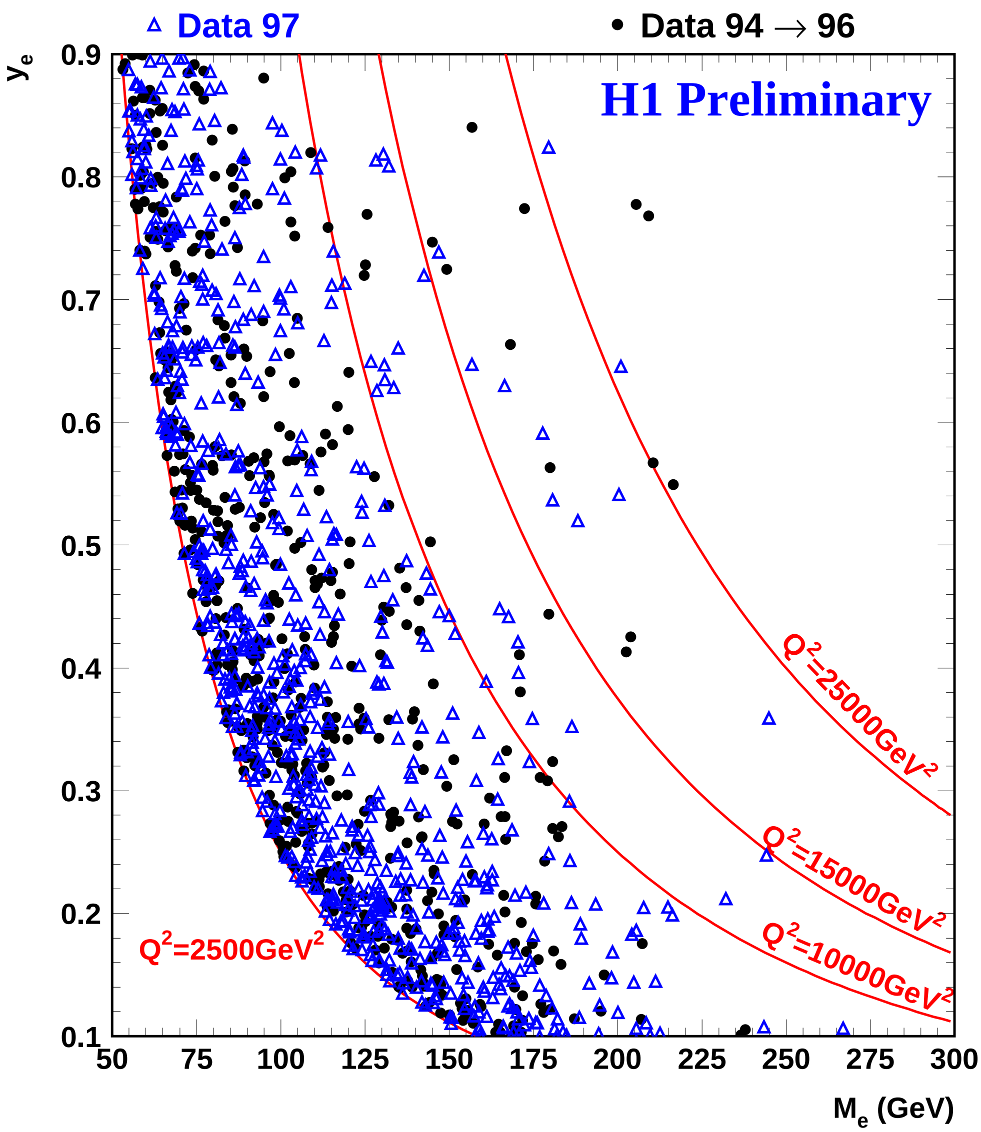

$Q_e^2 > 15000\text{GeV}^2$

$$\text{Obs.} = 22 \;\Leftrightarrow\; \text{Exp.} = 14.7 \pm 2.1$$

$M_e = 200 \pm 12.5$ GeV

$$\text{Obs} = 8 \text{ for 94-97} \;\Leftrightarrow\; \text{Exp} = 3.01 \pm 0.54$$

$$(\text{Obs} = 7 \text{ for 94-96} \;\Leftrightarrow\; \text{Exp} = 0.95 \pm 0.18)$$

accumulation of events in mass window is not confirmed by the 97 data (details → M.-C. Cousinou)

Q^2 Dependence

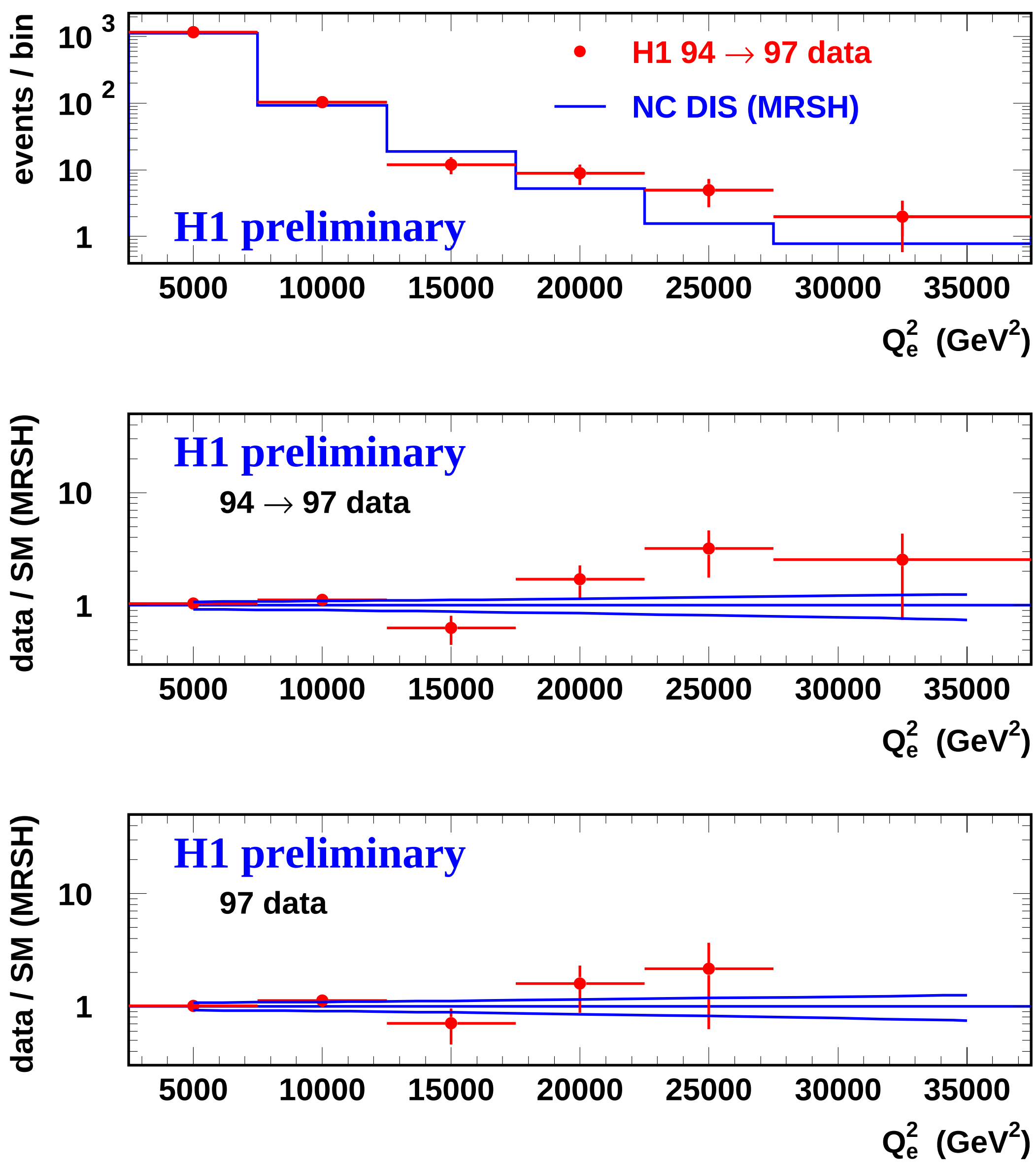

- Slight deviations from SM expectation observed for $Q_e^2 \gtrsim 15000 \mathrm{GeV}^2$
- Excess at highest Q_e^2 less significant than with 1994→96 data only

Cross Sections for $\boldsymbol{e^+p \rightarrow e^+X}$ at High $\boldsymbol{Q^2}$

Kinematic Domain: $200\ \mathrm{GeV}^2 \leq \mathrm{Q}^2 \leq 30000\ \mathrm{GeV}^2$

$0.005 \leq x \leq 0.65$

$$\frac{d^2\sigma}{dx\, dQ^2} = \frac{2\pi\alpha^2}{xQ^4}\left[Y_+F_2(x,Q^2) - y^2F_L(x,Q^2) - Y_-xF_3(x,Q^2)\right]$$

$$Y_\pm(y) = 1 \pm (1 \Leftrightarrow y)^2$$

F_2: generalized structure function
F_L: longitudinal structure function
F_3: parity violating term from Z° exchange

$$F_2 = F_2^{em} + \frac{Q^2}{(Q^2+M_Z^2)}F_2^{int} + \frac{Q^4}{(Q^2+M_Z^2)^2}F_2^{wk} = F_2^{em}(1+\delta_Z)$$

F_2^{em}: photon exchange
F_2^{wk}: Z° exchange
F_2^{int}: γZ° interference

- contributions from Z exchange and γZ interference terms only for $Q^2 > 1500\ \mathrm{GeV}^2$ at high y (low x)
- small influence of $F_L < 5\%$ at highest y values

In the following we will use the Reduced Cross Section:

$$\sigma(e^+p) \equiv \frac{xQ^4}{2\pi\alpha^2}\frac{1}{Y_+}\frac{\mathrm{d}^2\sigma}{\mathrm{d}x\mathrm{d}Q^2}$$

Neutral Current measurement at High Q^2

Event Selection of High Q^2 events:

- Calorimetric based trigger ($\epsilon > 99.5\%$)
- $E_e > 11$ GeV $\quad y_e < 0.9 \quad \theta_e \leq 150°$
- $|z_{vertex}| < 35$ cm
- $E\text{-}P_z > 35$ GeV

$\Rightarrow$ Data sample $\simeq$ 75000 events

$\Rightarrow$ Background $< 1\%$

extension of phase space to higher Q^2 and higher x

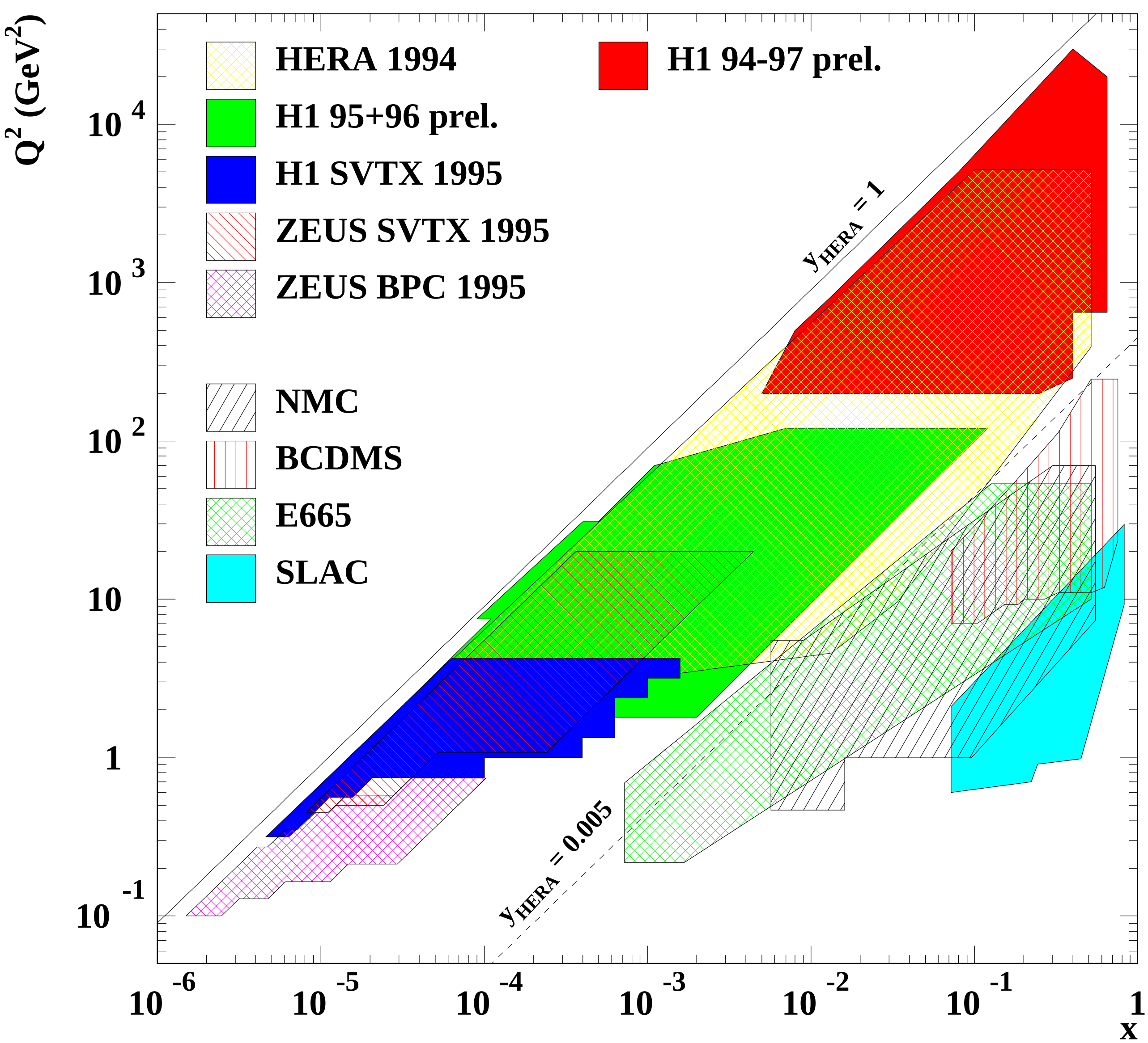

Sample of NC events

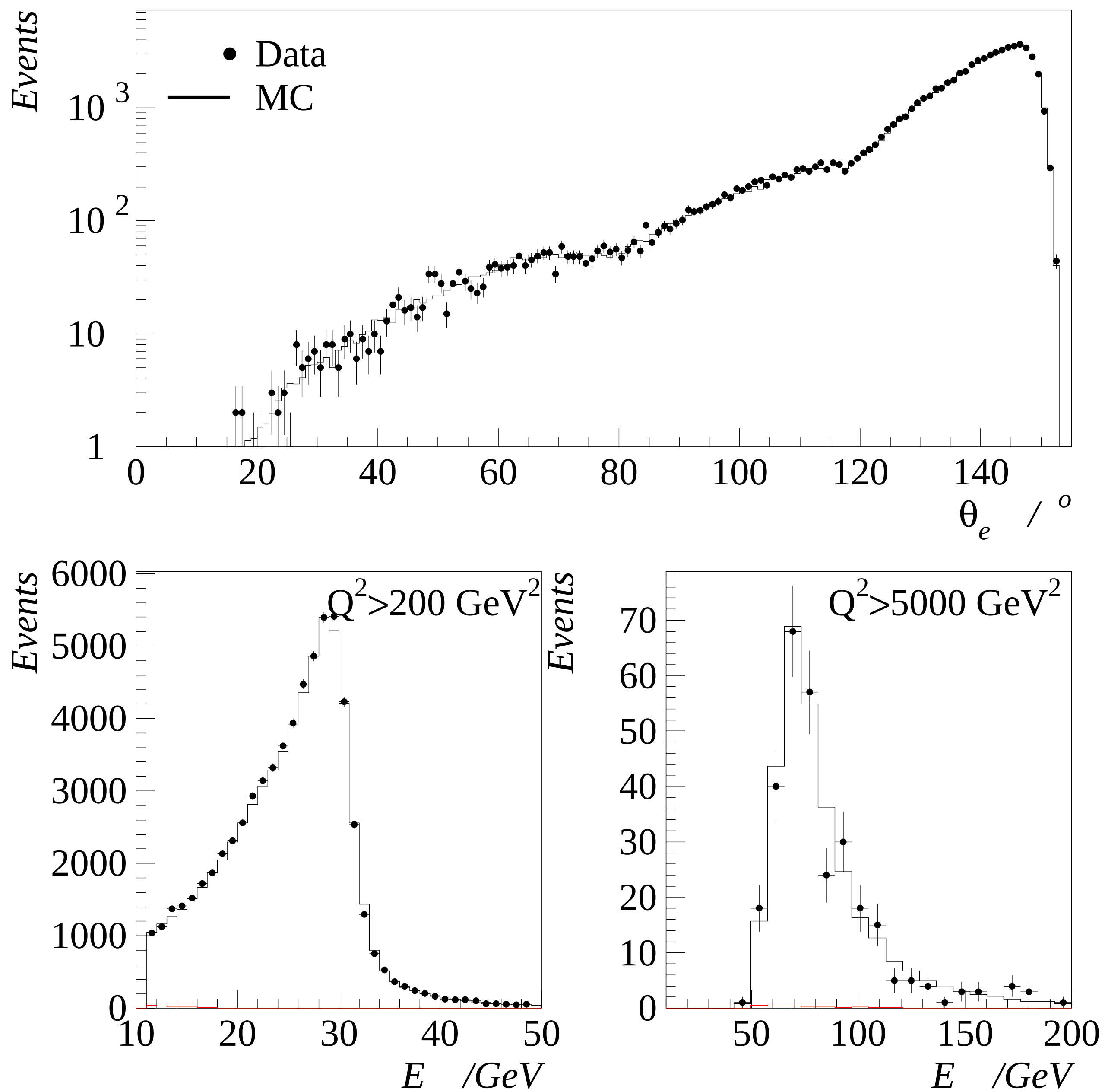

- Polar angle well described over the full Q^2 range ($\delta\theta \simeq 3$mrad)
- Energy spectrum under control in high Q^2 ($\delta \simeq 3\%$) and low Q^2 ($\delta \simeq 1\%$) region

Systematic Uncertainties for NC measurement

- main error sources
  - Trigger efficiency $\pm 0.5\%$
  - Electron finding efficiency $\pm 1\%$
  - e^+ Track validation $\pm 1\%$
  - Electron Energy scale $\pm 1 \Leftrightarrow 3\%$
  - e^+ scattering angle ± 3 mrad
  - Hadronic Energy scale $\pm 4\%$
  - Noise suppression $\pm 25\%$
  - Photoproduction background $\pm 30\%$
  - radiative corrections $\pm 2\%$
- no single error source dominates at low $Q^2 \approx 400$ GeV^2
- precision still limited statistical error for $Q^2 > 1000$ GeV^2

Comparison of e and Σ Method

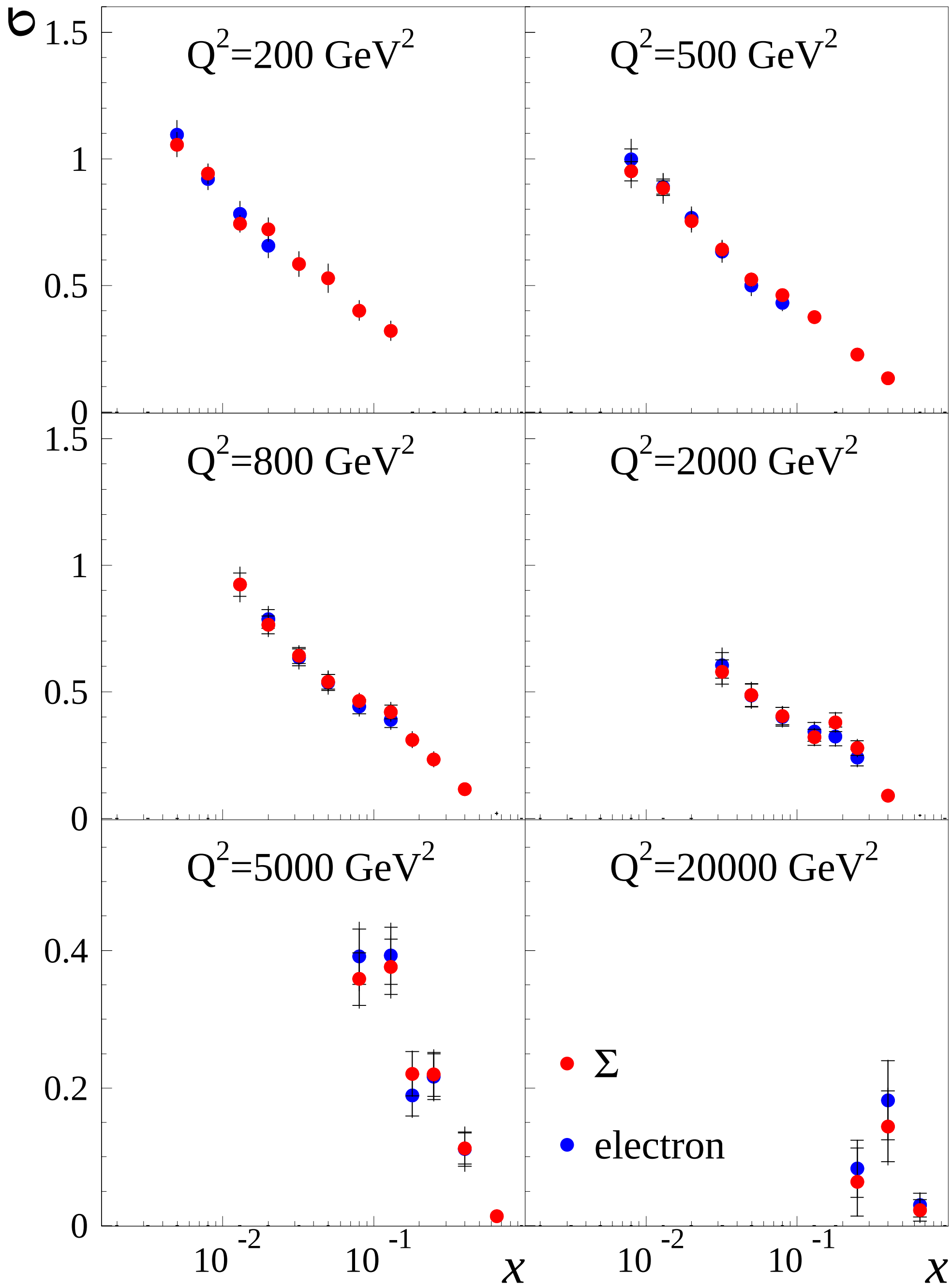

- Opposite systematic shift for electron energy error $\Rightarrow$ energy calibration check
- Different behaviour for radiative corrections
- For final result we use the $e\Sigma$-method (x_Σ, Q_e^2) which has a good stability in the full kinematic plane (cf DESY-97-137).

Reduced Cross Section

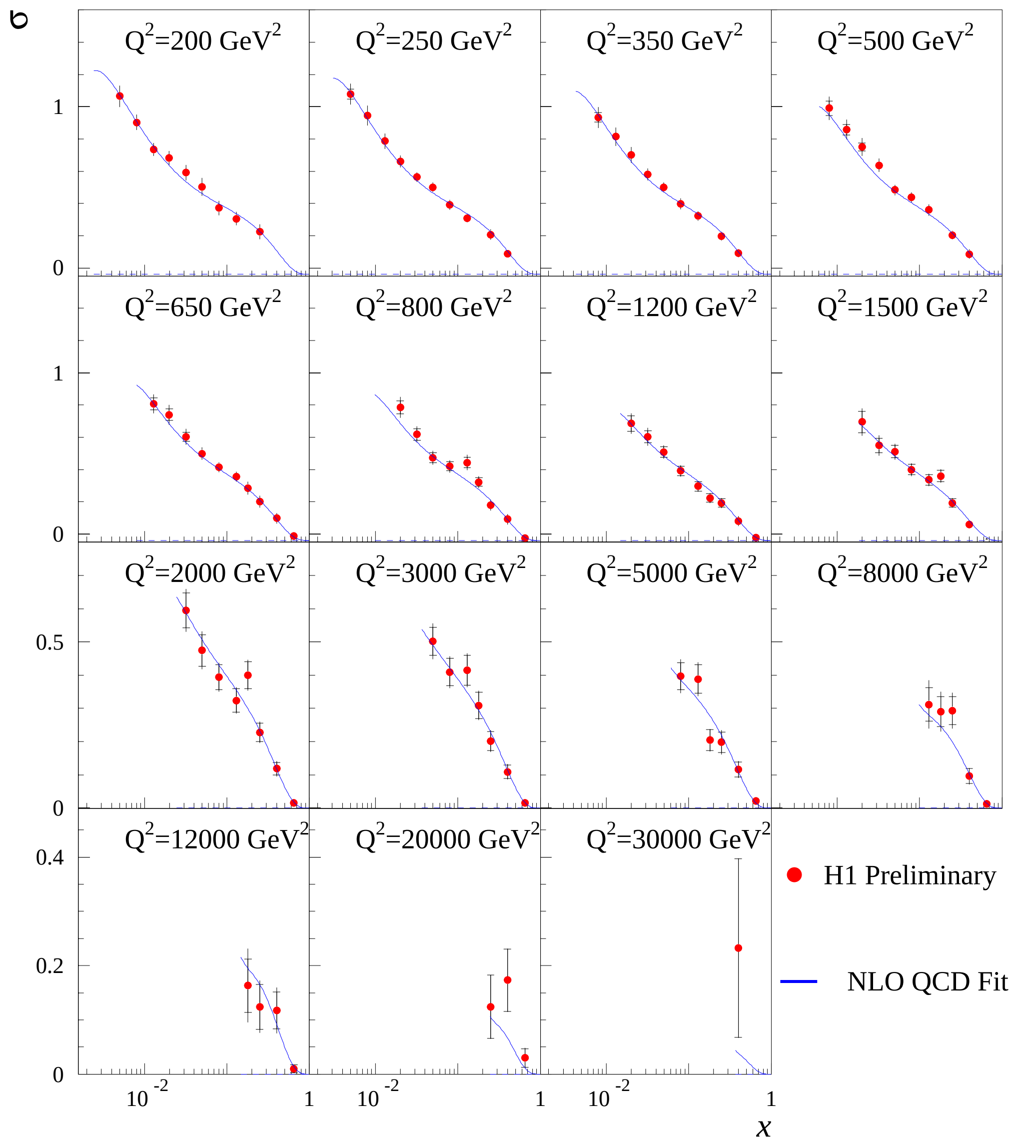

- Measurement from $Q^2 = 200$ to 30000 GeV^2. Up to $x = 0.65$ for $Q^2 \geq 650$ GeV^2
- NLO QCD fit gives good description of the data in the whole Q^2 and x range (details E. Rizvi)

Reduced Cross-section at High x

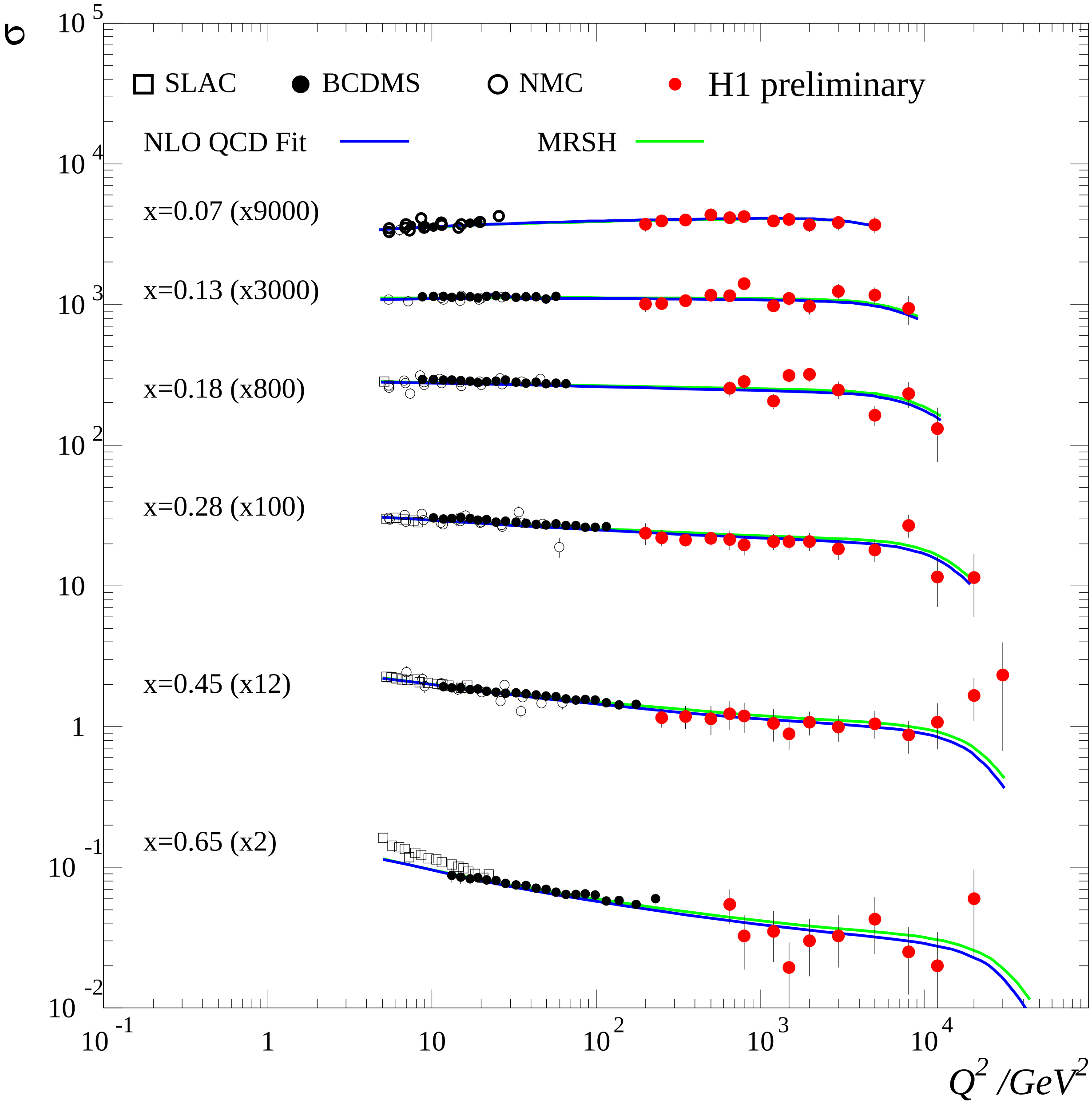

- approaching overlap with fixed target data at high x
- cross section falls at high x (scaling violation)
- high Q^2 HERA data now also have an influence at high x.

Single Differential Cross-Sections

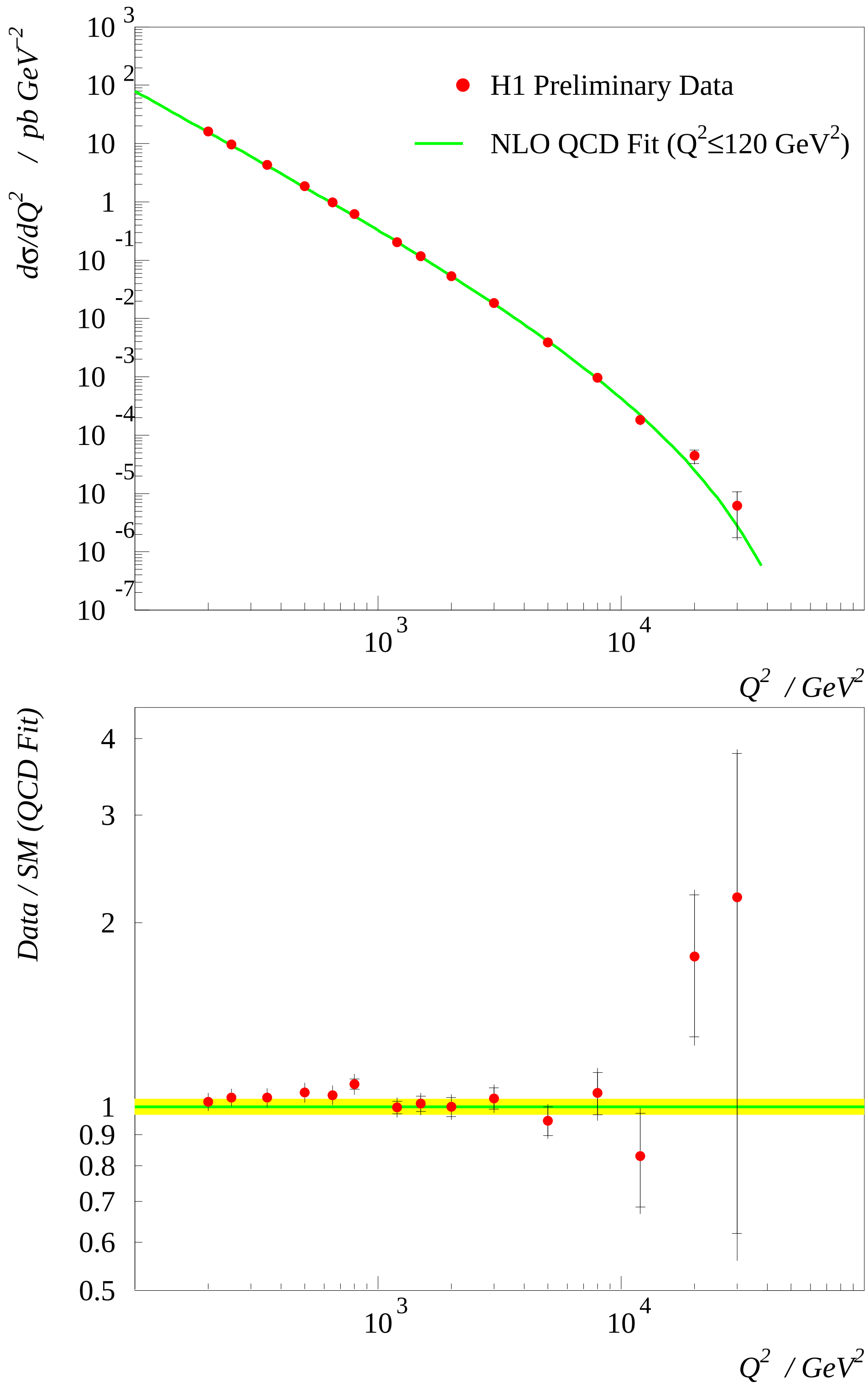

$\frac{\delta \mathcal{L}}{\mathcal{L}} = \pm 2.6$ %

- Neutral Current cross section falls by seven orders of magnitude in measured region
- High Q^2 data are compatible with a NLO QCD fit to all low Q^2 data ($\leq 120\mathrm{GeV}^2$) evolved over two orders of magnitude.
- Slight Excess visible at $Q^2 \geq 15000$ GeV^2.

Sensitivity To Z^0 Contribution

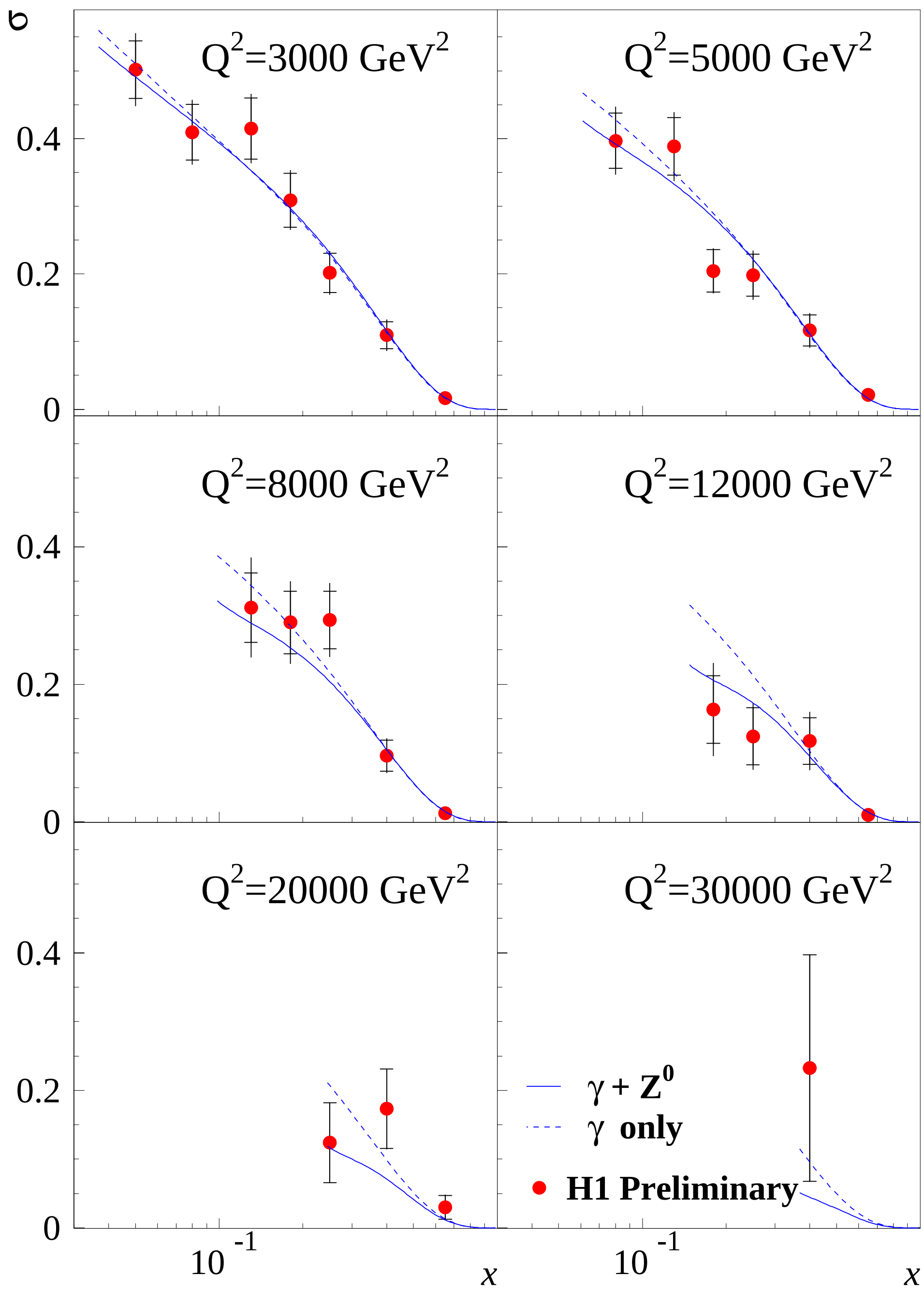

- Cross section reduced due to γZ interference at low x (high y)
- Effects are visible at $Q^2 \geq$10000 GeV^2
- Greater sensitivity can be gained from single differential distributions

$\mathrm{d}\boldsymbol{\sigma}/\mathrm{d}\boldsymbol{x}$ at $Q^2 > 1000, 10000\ \mathrm{GeV}^2$

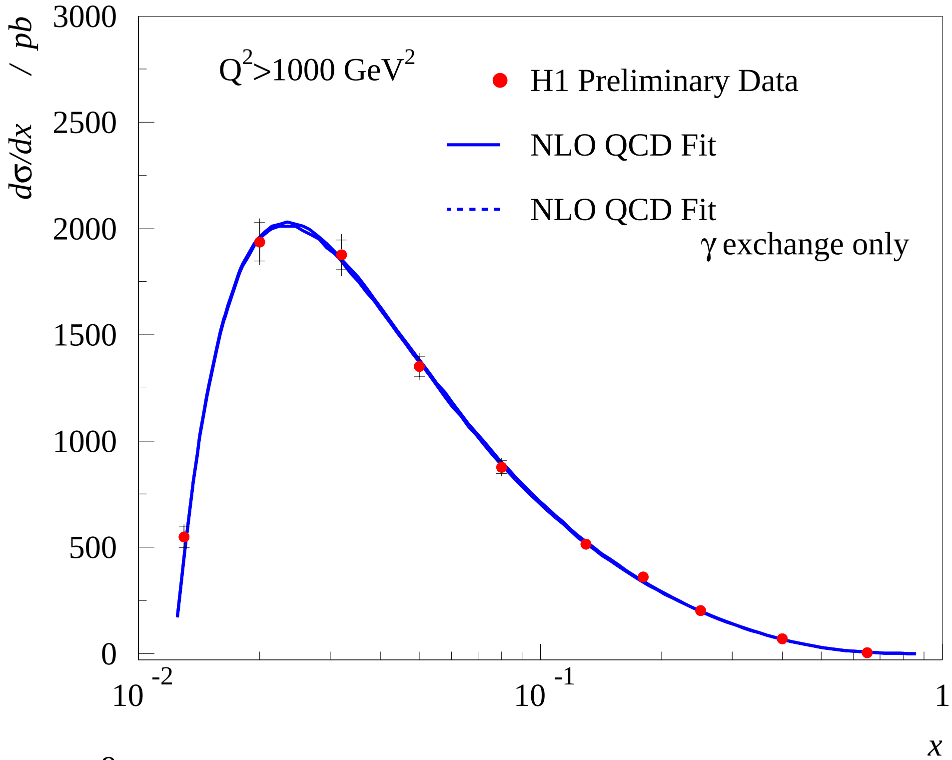

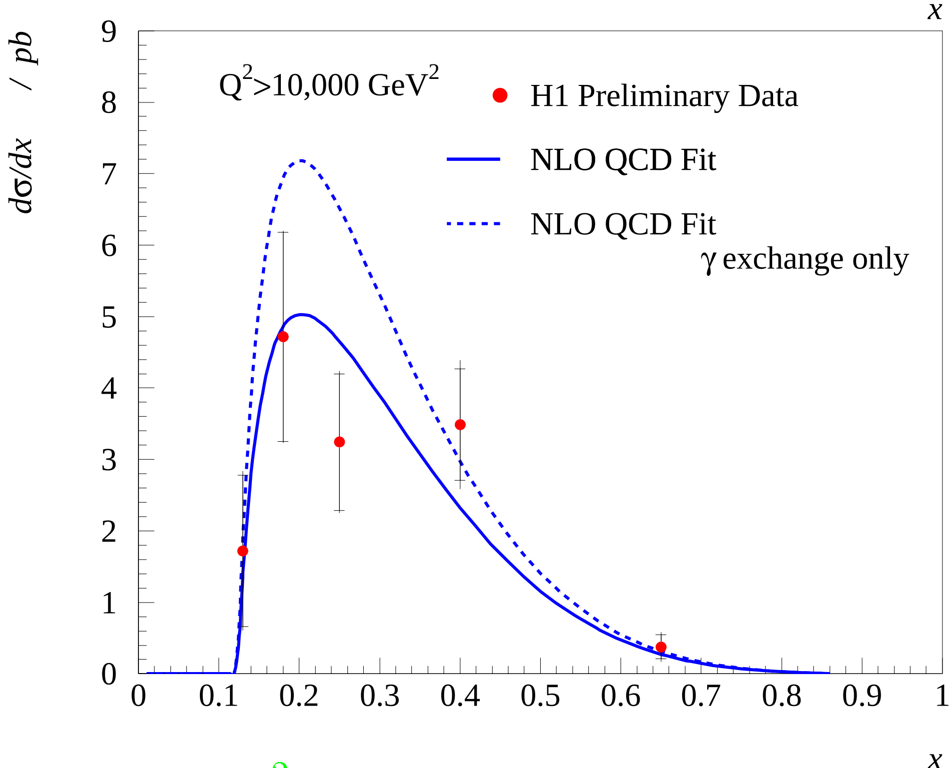

- For $Q^2 \geq 1000\ \mathrm{GeV}^2$, the cross-section is still dominated by low x partons.
- For $Q^2 \geq 10000\ \mathrm{GeV}^2$ the valence quarks contribute.
- The data are in good agreement with the electroweak Standard Model.

Charged Current Deep Inelastic Scattering

Cross Section for $e^+p \longrightarrow \bar{\nu}X$:

$$\frac{d^2\sigma}{dxdQ^2} = \frac{G_F^2}{2\pi}\frac{1}{(1+Q^2/m_W^2)^2}\left(\bar{u}+\bar{c}+(1 \Leftrightarrow y)^2(d+s)\right)$$

- Propagator ⇒ W mass determination
  (94: 85^{+9+5}_{-6-4} GeV)
- parton densities ⇒ sensitivity to d-quark density
- helicity dependence ⇒ V-A coupling

Radiative Corrections ($< 10\%$) depend on M_W ⇒
Measure radiative Cross Section
We define the

Reduced Charged Current Cross Section:

$$\begin{aligned}\sigma_{CC} &\equiv x \cdot \frac{2\pi}{G_F^2}(1+Q^2/m_W^2)^2\frac{d^2\sigma}{dxdQ^2} \\ &= x \cdot (\bar{u}+\bar{c}+(1-y)^2(d+s))\end{aligned}$$

in Standard Model

- definition in analogy to Reduced Neutral Current Cross Section σ
- measurement of the parton densities

Selection of Charged Current Events

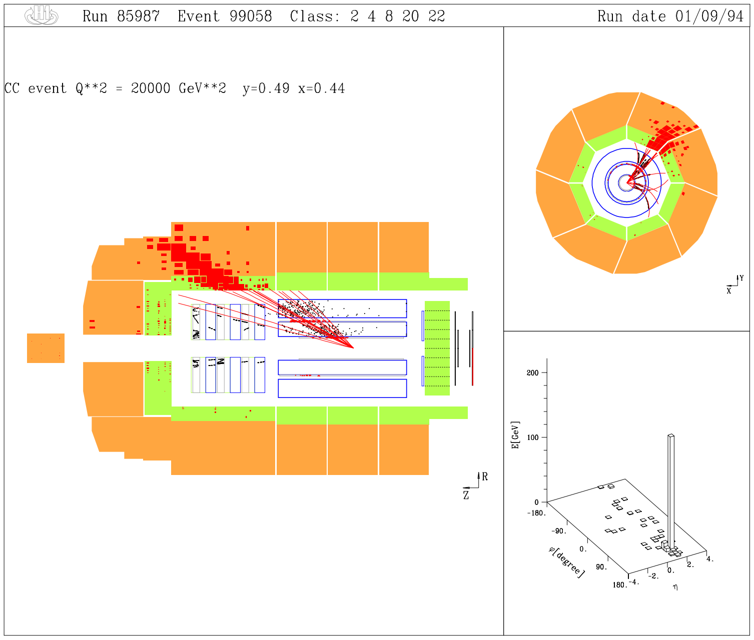

- Calorimeter and track based trigger $\Longrightarrow$ $\epsilon = 50 - 100\%$ depending on P_t
- $P_t > 12$ GeV
- $z_{vtx} < 35$ cm
- topological Non-ep-background filters
- γp background: $P_{t,antiparallel}/P_{t,parallel} < 0.15$
- reconstruction of kinematic variables from tracks and calorimetris energy depositions
- good understanding of hadronic energy scale essential

Single differential Charged Current Cross Section

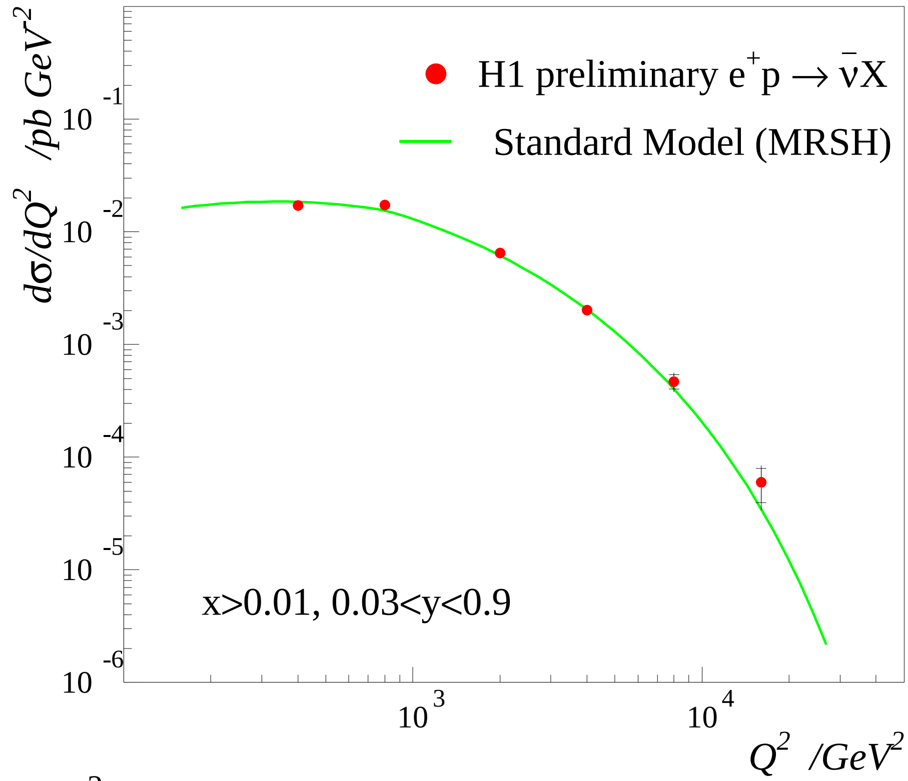

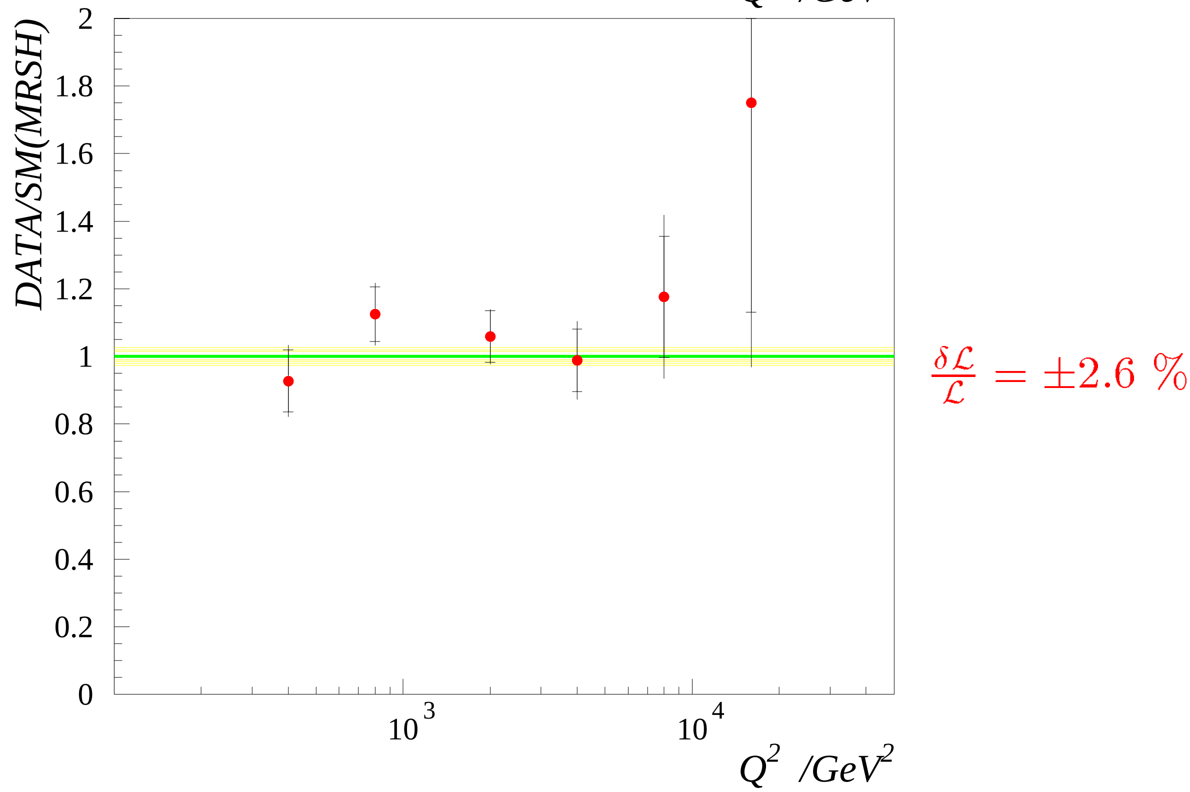

- shape of cross section determined by propagator mass
- statistical errors dominate

Neutral and Charged Current Cross Section

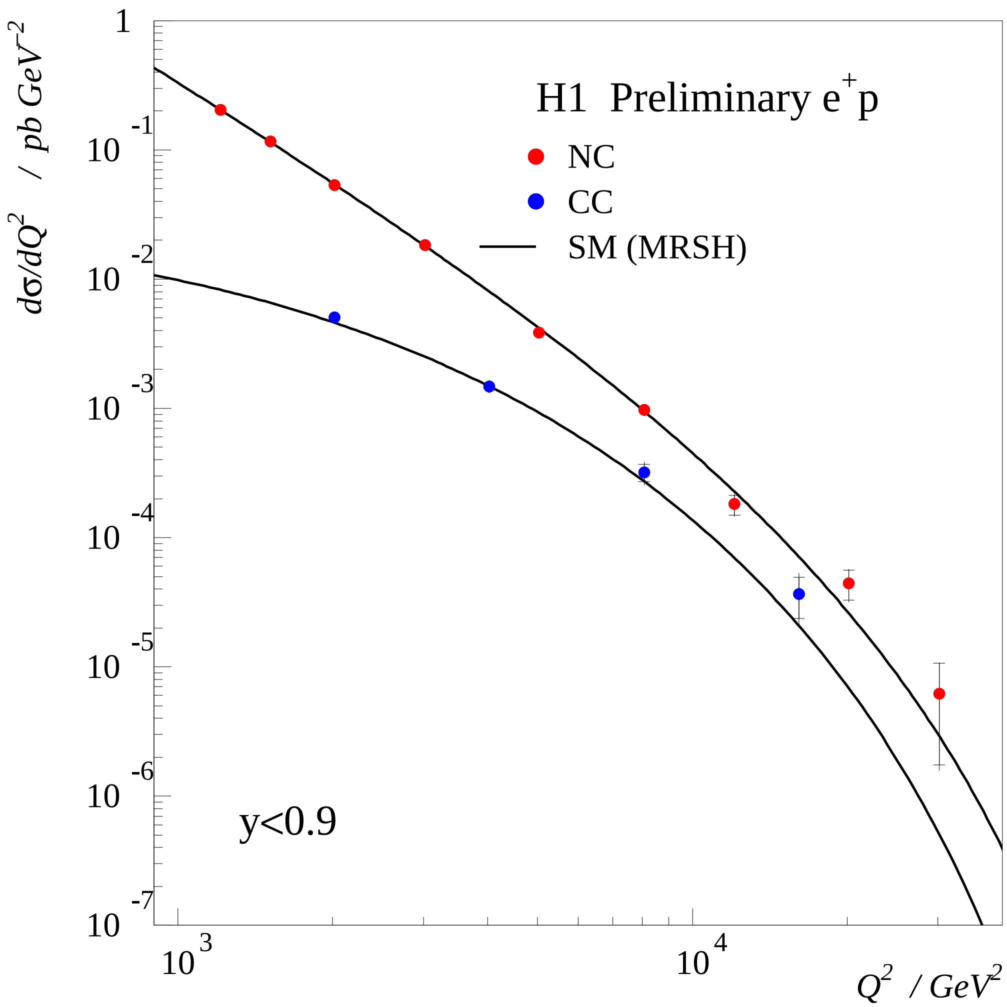

- Neutral and Charged Current cross section approaching each other with increasing Q^2 as expected from Standard Model
- remaining difference at high Q^2 due to coupling to different quark flavours

Comparison of Reduced NC Cross Section between "hadron" and "electron" method

- important cross check of hadronic energy scale control

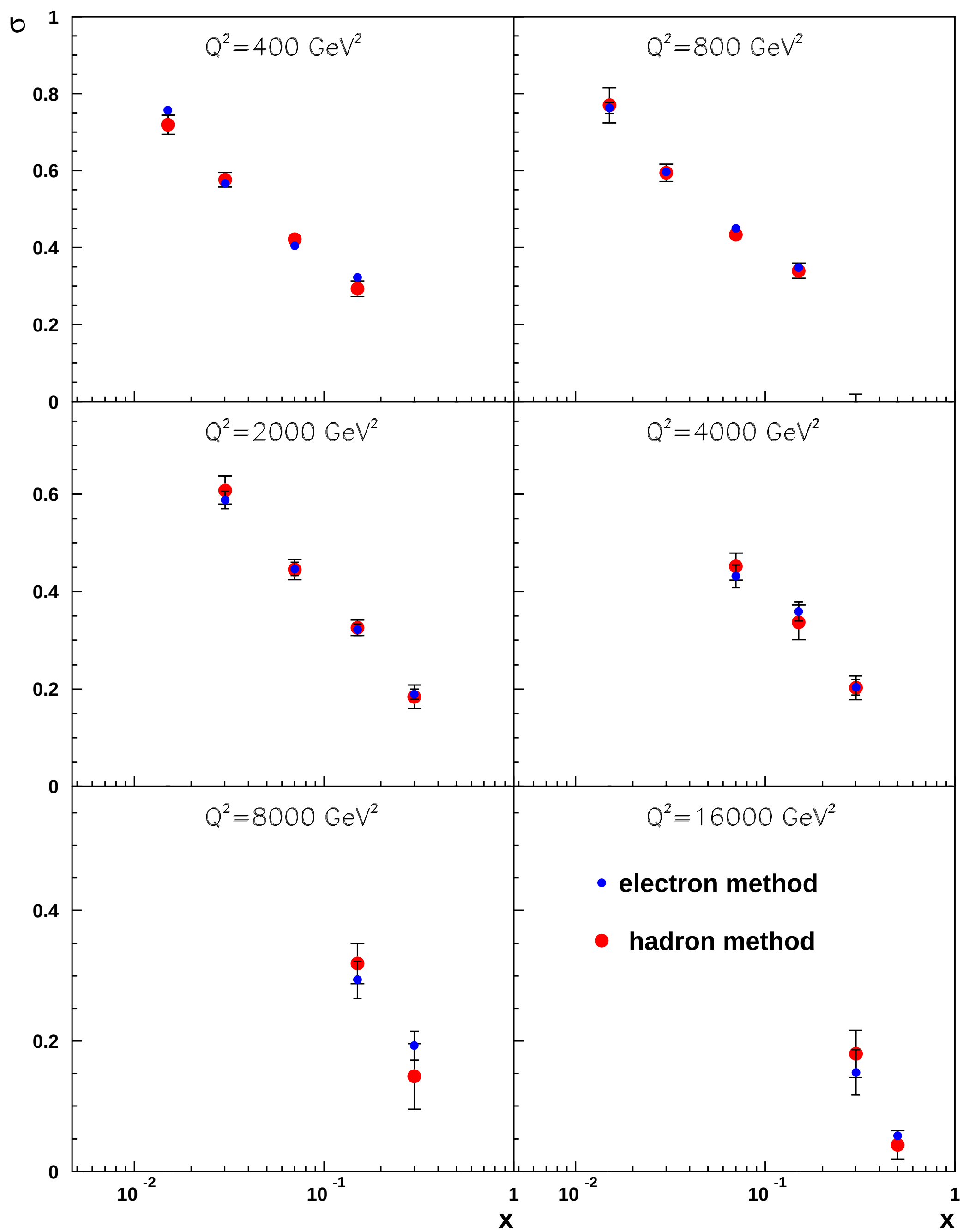

- electron and hadron method agree within systematic errors only
- hadronic energy scale well known in terms of x and Q^2

Systematic Uncertainties for CC measurement

main error sources

- Trigger efficiency $(1 \Leftrightarrow \epsilon) * 10\%$
- Vertex Efficiency $\approx \pm 1\%$
- Hadronic Energy scale $\pm 4\%$
- Noise suppression $\pm 25\%$
- Photoproduction background $\pm 50\%$

error on hadronic energy scale dominating

Reduced Charged Current Cross Section

$$\sigma_{CC} \equiv \frac{2\pi}{G_F^2}\left[\frac{(M_W^2+Q^2)}{M_W^2}\right]^2 \cdot x \cdot \frac{d^2\sigma}{dxdQ^2}$$

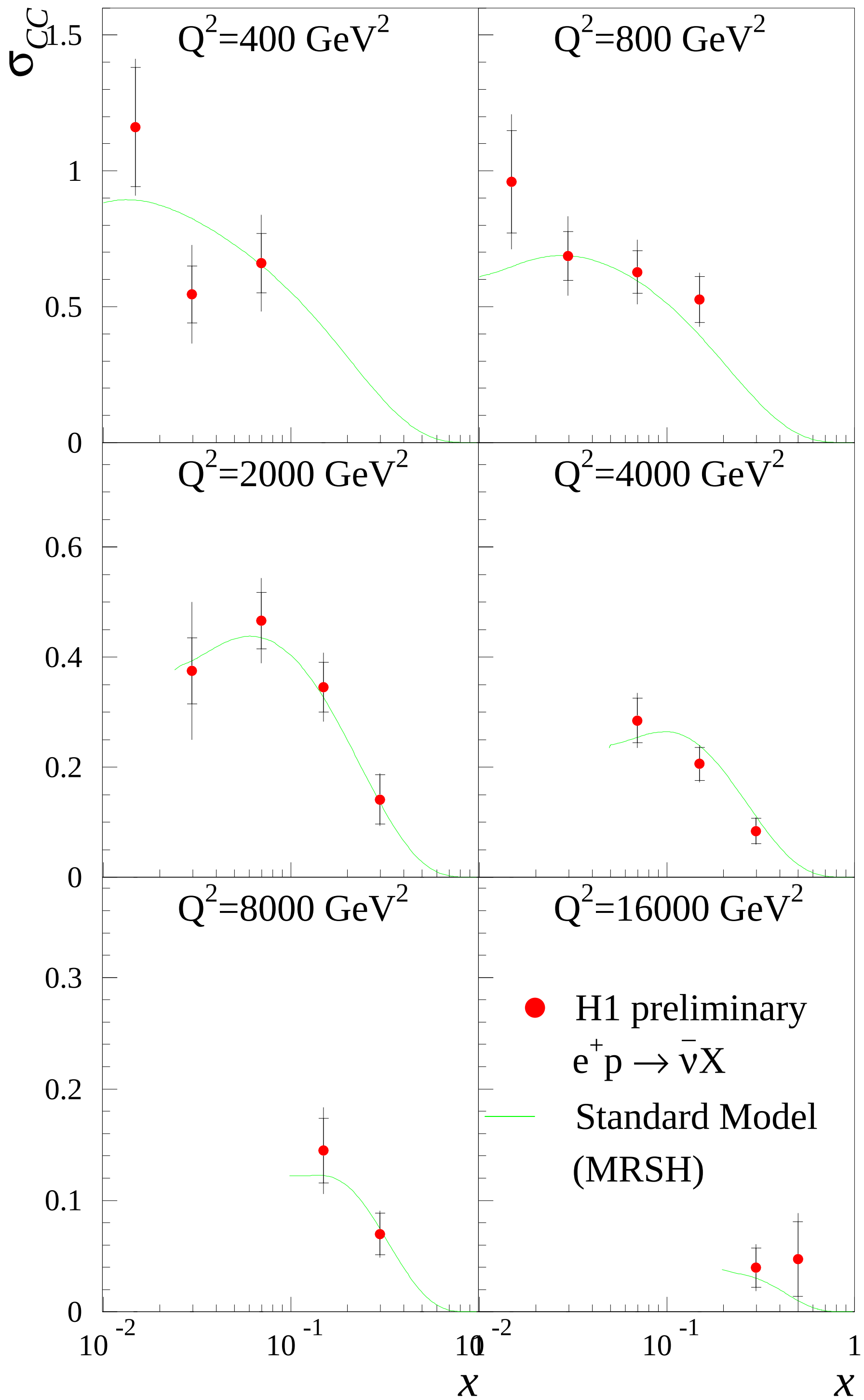

- double differential measurement at high x and high Q^2
- good agreement with Standard Model prediction

Quark and Antiquark Contributions to CC Cross Section

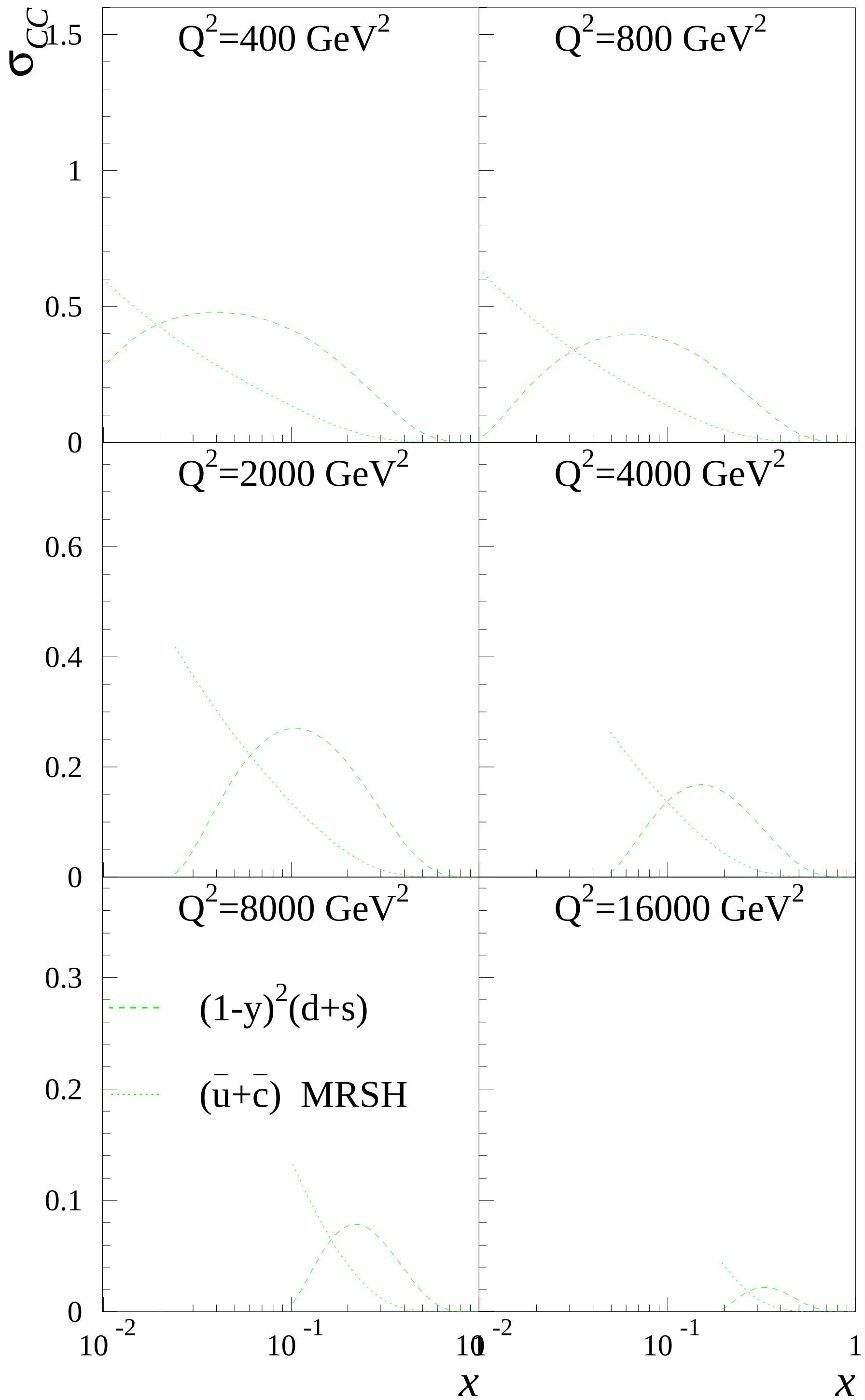

- sensitivity to quark and antiquark densities at high Q^2

Comparison of Reduced CC and NC Cross Section

Coupling to different quarks in Neutral and Charged Current interaction (QPM):

$$\begin{aligned}
\text{NC: } \sigma_{NC} &= x \cdot \left[\frac{4}{9}(u + \bar{u} + c + \bar{c}) + \frac{1}{9}(d + \bar{d} + s + \bar{s})\right](1 + \delta_{Z,L}) \\
\text{CC: } \sigma_{CC} &= x \cdot \left[\bar{u} + \bar{c} + (1 \Leftrightarrow y)^2 (d + s)\right]
\end{aligned}$$

$\Rightarrow$

- Main contribution to NC cross section from u type quarks
- CC Cross section at high y mainly determined by $\bar{u}$ and at low y mainly determined by d

use helicity dependence to estimate antiquark and quark contribution to Charged Current cross section

– neglect contribution from c, s and d in NC

– compare

$$\begin{aligned}
(1 \Leftrightarrow y)^2 \cdot \sigma_{NC} &\approx (1 \Leftrightarrow y)^2 \frac{4}{9} \; x\,(u_v + u_{sea} + \bar{u}) \\
\sigma_{CC} &\approx (1 \Leftrightarrow y)^2 \; x\, d_v \quad + \quad x\,(\bar{u} + \bar{c})
\end{aligned}$$

– $(1 - y)^2 \sigma_{NC} / \sigma_{CC} \approx \frac{4}{9} u_v / d_v$ at high x (low y)

– see antiquark density $\bar{u}$ at low x

Warning: This is only a qualitative comparison!

Weighted NC and CC Cross Section

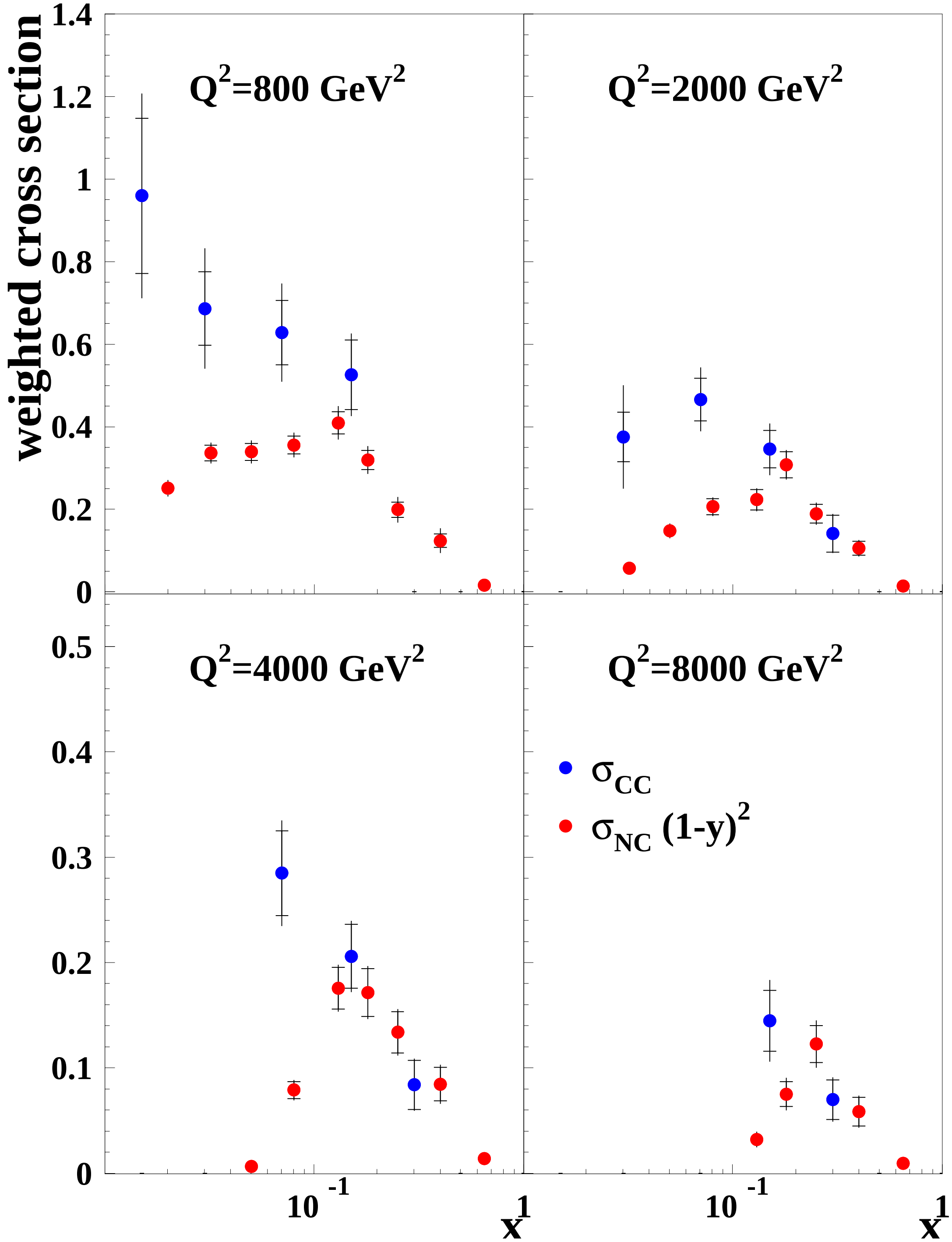

- relation between NC and CC cross section as expected from QPM
- measurement of d quark density and d/u ratio at high Q^2 will be done

Summary

- The excess of neutral current events observed at high Q^2 in the 94-96 data is still present, but with a lower significance ($\simeq 2\sigma$ at $Q^2 \geq 15000$ GeV^2 for the data taken from 94 to 97).
- Single and double differential Neutral Current cross-sections have been measured for Q^2 from 200 to 30000 GeV^2, in the valence region up to $x = 0.65$ with a precision comparable to the low Q^2 HERA data.
- These cross-section measurements are very well described over two orders of magnitude in Q^2 by perturbative QCD, as shown by a Next to Leading Order QCD fit
- At high Q^2 (≥ 10000 GeV^2), the single differential $d\sigma/dx$ cross-section favours the Standard Model expectation of a suppression of the cross-section due to $\gamma \Leftrightarrow Z^0$ interference.
- The single differential Charged Current cross sections shows the Q^2 dependence as expected from the Standard Model
- The double differential Charged Current cross section has been measured for $Q^2 = 400 \Leftrightarrow 16000$ GeV^2 and $x = 0.01 \Leftrightarrow 0.5$ and covers the regions where valence- and the region where sea- quarks dominate
- We are looking forward to e^-p data taking this year!